On competitive gas adsorption and absorption phenomena in thin films of ionic liquids

(Supplementary information)

Dmitry N. Lapshin*[a], Miguel Jorge[b], Eleanor E. B. Campbell[c,d], Lev Sarkisov[e]

*[a] Institute for Materials and Processes, School of Engineering, University of Edinburgh, Robert Stevenson Road, Edinburgh EH9 3FB, United Kingdom. E-mail: Dmitry.Lapshin@ed.ac.uk.

[b] Department of Chemical and Process Engineering, University of Strathclyde, 75 Montrose Street, Glasgow G1 1XJ, United Kingdom.

[c] EaStCHEM, School of Chemistry, University of Edinburgh, David Brewster Road, Edinburgh EH9 3FJ, United Kingdom.

[d] School of Physics, Konkuk University, Seoul 05029, South Korea.

[e] Department of Chemical Engineering and Analytical Science, School of Engineering, University of Manchester, Manchester M13 9PL, United Kingdom.

Contents

1. Simulated systems

All simulations for this work have been conducted at four different temperatures, in particular, 298, 323, 343, and 393 K. All systems listed in Table S1 have the same cell size along the *x*- and *y*-axes equal to 5.64 nm and contain the same number of ion-pairs equal to 500.

Table S1. Simulated systems of binary and ternary mixtures of ionic liquid, $[BMIM]^+[PF_6]^-$, and gas.

#	*T*, *K*	Composition of the gas phase, x_{CO2}	Total gas pressure, *P*, *MPa*	Box size along *z*-axis, *nm*	Number of gas molecules	
					CO_2	N_2
1	298	1.000	0.0925	120.720	100	0
2		1.000	0.229	38.000	100	0
3		1.000	0.350	18.581	100	0
4		1.000	0.510	31.521	200	0
5		1.000	0.632	31.521	250	0
6		1.000	0.889	31.521	350	0
7		0.000	0.110	120.720	0	100
8		0.000	0.373	38.000	0	100
9		0.000	0.869	18.581	0	100
10		0.439	0.196	120.720	100	100
11		0.371	0.599	38.000	100	100
12		0.291	1.242	18.581	100	100
13		0.357	1.451	31.521	200	200
14		0.358	1.818	31.521	250	250
15		0.356	2.538	31.521	350	350
16	323	1.000	0.105	120.720	100	0
17		1.000	0.285	38.000	100	0
18		1.000	0.468	18.581	100	0
19		1.000	0.655	31.521	200	0
20		1.000	0.809	31.521	250	0
21		1.000	1.113	31.521	350	0
22		0.467	0.218	120.720	100	100
23		0.409	0.691	38.000	100	100
24		0.325	1.456	18.581	100	100
25		0.390	1.671	31.521	200	200
26		0.387	2.095	31.521	250	250
27		0.382	2.948	31.521	350	350
28	343	1.000	0.115	120.720	100	0
29		1.000	0.326	38.000	100	0
30		1.000	0.566	18.581	100	0
31		1.000	0.747	31.521	200	0
32		1.000	0.944	31.521	250	0
33		1.000	1.296	31.521	350	0
34		0.468	0.240	120.720	100	100
35		0.420	0.760	38.000	100	100
36		0.355	1.636	18.581	100	100
37		0.410	1.854	31.521	200	200
38		0.408	2.326	31.521	250	250
39		0.403	3.224	31.521	350	350
40	393	1.000	0.136	120.720	100	0
41		1.000	0.420	38.000	100	0
42		1.000	0.812	18.581	100	0

Table S1 (*continued*)

43	1.000	0.991	31.521	200	0
44	1.000	1.229	31.521	250	0
45	1.000	1.712	31.521	350	0
46	0.477	0.281	120.720	100	100
47	0.449	0.930	38.000	100	100
48	0.399	2.076	18.581	100	100
49	0.437	2.276	31.521	200	200
50	0.437	2.852	31.521	250	250
51	0.434	3.965	31.521	350	350

2. Validation of simulation results for bulk ionic liquid

Table S2 provides key results that we use to validate our simulations and the accuracy of the chosen force field parameters provided by Doherty et al.[1] in describing key physical properties of the bulk ionic liquid, $[BMIM]^+[PF_6]^-$. These results can be summarized as follows. Typical properties of bulk ionic liquids explored in the literature are density, surface tension, and self-diffusion coefficient. The density of the simulated $[BMIM]^+[PF_6]^-$ at 298.15 K agrees with the reported value of 1315 kg/m^3. The surface tension and ion self-diffusion coefficients obtained at 425.15 K are also in agreement with the reference simulation. Moreover, the simulation results are in good agreement with the experimental results for both temperatures.

Table S2. Properties of $[BMIM]^+[PF_6]^-$, obtained from computational and experimental studies.

Force field	*T*, *K*	Density, *g/cm³*	Surface tension, *mN/m*	Self-diffusion coefficient, $D \cdot 10^{11}$ *m²/s*	
				Cation	Anion
This study	298	1.315	46.3	0.551	0.335
0.8*OPLS	425	1.194	30.2	30.1	26.2
Reference	298	1.315	n/a	n/a	n/a
0.8*OPLS[1]	425	n/a	36.4	29.5	26.2
Experiment	298	1.367[2]	43.8[c]	0.720[b]	0.524[b]
	425	1.262[a]	35.9	31.8[b]	27.9[b]

[a] – extrapolated using experimental data of Fan et al.[2]; [b] – Vogel-Fulcher-Tamman equation using Tokuda et al. experimental parameters[3]; c - extrapolated using experimental data of Freire et al.[4]

3. Simulation details

Molecular Dynamics simulations were performed using the Gromacs simulation package (v.5.1.2).[5] Each simulation was performed in three steps: energy minimization (1 ns), equilibration (10 ns) and production run (55 ns). Prior to simulating gas-liquid interfacial systems in the Canonical ensemble, a cubic box containing 500 ion pairs of $[BMIM]^+[PF_6]^-$ was generated using Packmol software package.[6] This initial configuration of the pure ionic liquid was minimized using the steepest descent algorithm for 1 ns (parameters are provided in commented `ENERGY MINIMIZATION OPTIONS` section, Table S3), equilibrated in the Canonical ensemble for 1 ns and in the isobaric-isothermal ensemble for 2 ns, followed by the production run for 6 ns (additional parameters used for NPT simulations are provided in commented `Pressure coupling` section, Table S3). The final configuration of the cubic box of the ionic liquid thus generated was used in all simulations of gas-liquid interfacial systems. In Table S3 we summarize all simulation details for interfacial systems. Simulation details for the bulk ionic liquid systems are identical to those of the original article by Doherty *et al.*[1], and are not repeated here. Files required to carry out all simulations are provided, see the link

https://github.com/SarkisovGroup/Interfaces.git

Table S3. Key simulation parameters for interfacial systems, `*.mdp` file.

```
; RUN CONTROL PARAMETERS  ;l_bfgs
integrator               = md
; Start time and timestep in ps
tinit                    = 0
dt                       = 0.001
nsteps                   = 55000000
; mode for center of mass motion removal
comm-mode                = linear
; number of steps for center of mass motion removal
nstcomm                  = 10
; group(s) for center of mass motion removal

; ENERGY MINIMIZATION OPTIONS (this is used prior to equilibration)
; Force tolerance and initial step-size
; emtol                  = 100
; emstep                 = 0.001
; Frequency of steepest descents steps when doing CG
; nstcgsteep             = 5000
; nbfgscorr              = 10

; NEIGHBORSEARCHING PARAMETERS
; nblist update frequency
nstlist                  = 10
cutoff-scheme            = Verlet
; ns algorithm (simple or grid)
ns-type                  = grid
; Periodic boundary conditions: xyz (default), no (vacuum)
; or full (infinite systems only)
pbc                      = xyz
; nblist cut-off
rlist                    = 1.3

; OPTIONS FOR ELECTROSTATICS AND VDW
; Method for doing electrostatics
coulombtype              = PME
rcoulomb-switch          = 0
```

```
rcoulomb                 = 1.3
; Dielectric constant (DC) for cut-off or DC of reaction field
epsilon_rf               =
; Method for doing Van der Waals
vdw-type                 = cutoff
; cut-off lengths
rvdw-switch              =
rvdw                     = 1.3
; Apply long range dispersion corrections for Energy and Pressure
DispCorr                 = EnerPres
; Extension of the potential lookup tables beyond the cut-off
table-extension          = 1
; Spacing for the PME/PPPM FFT grid
fourierspacing           = 0.1
; FFT grid size, when a value is 0 fourierspacing will be used
fourier_nx               = 0
fourier_ny               = 0
fourier_nz               = 0
; EWALD/PME/PPPM parameters
pme_order                = 4
ewald_rtol               = 1e-05
ewald_geometry           = 3d
epsilon_surface          = 0

; OPTIONS FOR WEAK COUPLING ALGORITHMS
; Temperature coupling
Tcoupl                   = V-rescale
; Groups to couple separately
tc-grps                  = System
; Time constant (ps) and reference temperature (K)
tau_t                    = 1.0
ref_t                    = 298.15
; Pressure coupling (this is used to simulate only bulk ionic liquid)
; Pcoupl                   = Berendsen
; Pcoupltype               = isotropic
; Time constant (ps), compressibility (1/bar) and reference P (bar)
; tau_p                    = 4.0
; compressibility          = 4.23e-5
; ref_p                    = 1.00

; OPTIONS FOR BONDS
constraints              = hbonds
constraint_algorithm     = LINCS
lincs-order              = 4
Lincs-iter               = 2
Lincs-warnangle          = 50
shake_tol                = 1e-5
```

4. Force field parameters

Fully flexible ions of ionic liquid were simulated using the non-polarizable OPLS-AA force field formalism.[1] Lennard-Jones parameters and partial charges for $[BMIM]^+[PF_6]^-$, CO_2 and N_2 are summarized in Table S4 and bonded parameters are reported in Tables S5-8. Lennard-Jones cross interactions between different atoms were calculated using geometric `Combination rule 3` according to the Gromacs convention, Equations (S1) and (S2). The 1,4-intramolecular interactions were reduced by a factor of 2.

$$\sigma_{ij} = \sqrt{\sigma_i \sigma_j} \tag{S1}$$

$$\varepsilon_{ij} = \sqrt{\varepsilon_i \varepsilon_j} \tag{S2}$$

Table S4. General OPLS-AA force field parameters, `oplsaa.itp` file.

```
[ atomtypes ]
; Type       mass    charge  ptype    sigma(nm) epsilon(kJ/mol)
; BMIM
    CR    12.0110    -0.072      A    0.355     0.292880
    NA    14.0067     0.176      A    0.325     0.711280
    CW    12.0110    -0.192      A    0.355     0.292880
    HR     1.0080     0.168      A    0.242     0.125520
    HW     1.0080     0.216      A    0.242     0.125520
    CM    12.0110    -0.280      A    0.350     0.276144
    HM     1.0080     0.144      A    0.250     0.125520
    CA    12.0110    -0.136      A    0.350     0.276144
    HA     1.0080     0.144      A    0.250     0.125520
    CS    12.0110    -0.096      A    0.350     0.276144
    HS     1.0080     0.048      A    0.250     0.125520
    CT    12.0110    -0.192      A    0.350     0.276144
    HT     1.0080     0.064      A    0.250     0.125520
; PF6
     P    30.9740     1.072      A    0.37400   0.837000
     F    18.9980    -0.312      A    0.31181   0.255220
; CO2
     C    12.0107     0.700      A    0.280     0.224490
     O    15.9994    -0.350      A    0.305     0.656842
; VIRTUAL SITES
    MW    0.00000     0.000      V    0.000     0.000000
; N2
     N    14.0067    -0.482      A    0.331     0.299214
```

Table S5. Bonded parameters for the cation, $[BMIM]^+$, `BMIM.itp` file.

```
    [  moleculetype  ]
;    name    nrexcl
     BMIM    3

    [  atoms  ]
;  nr    type resnr residu atom  cgnr   charge    mass
    1     NA    1    BMIM   N02    1    0.176     14.007
    2     NA    1    BMIM   N00    2    0.176     14.007
    3     CR    1    BMIM   C01    3   -0.072     12.011
    4     HR    1    BMIM   H07    3    0.168     1.008
    5     CW    1    BMIM   C04    4   -0.192     12.011
    6     HW    1    BMIM   H09    4    0.216     1.008
    7     CW    1    BMIM   C03    5   -0.192     12.011
    8     HW    1    BMIM   H08    5    0.216     1.008
    9     CM    1    BMIM   C05    6   -0.28      12.011
    10    HM    1    BMIM   H0B    6    0.144     1.008
    11    HM    1    BMIM   H0C    6    0.144     1.008
    12    HM    1    BMIM   H0D    6    0.144     1.008
    13    CA    1    BMIM   C06    7   -0.136     12.011
    14    HA    1    BMIM   H0E    7    0.144     1.008
    15    HA    1    BMIM   H0F    7    0.144     1.008
    16    CS    1    BMIM   C0G    8   -0.096     12.011
    17    HS    1    BMIM   H0H    8    0.048     1.008
    18    HS    1    BMIM   H0I    8    0.048     1.008
    19    CS    1    BMIM   C0J    9   -0.096     12.011
    20    HS    1    BMIM   H0K    9    0.048     1.008
    21    HS    1    BMIM   H0M    9    0.048     1.008
    22    CT    1    BMIM   C0N    10  -0.192     12.011
    23    HT    1    BMIM   H0O    10    0.064    1.008
    24    HT    1    BMIM   H0P    10    0.064    1.008
    25    HT    1    BMIM   H0Q    10    0.064    1.008
    [  bonds  ]
;   ai    aj  funct   c0(nm)     c1(kJ mol-1 nm-2)
    1     3     1    0.1315    399153.6 ; NA-CR
    1     5     1    0.1378    357313.6 ; NA-CW
    1     13    1    0.1476    282001.6 ; NA-CA
    2     3     1    0.1315    399153.6 ; NA-CR
    2     7     1    0.1378    357313.6 ; NA-CW
    2     9     1    0.1465    282001.6 ; NA-CM
    3     4     1    0.1069    307105.6 ; CR-HR
    5     6     1    0.1068    307105.6 ; CW-HW
    5     7     1    0.1336    435136.0 ; CW-CW
    7     8     1    0.1068    307105.6 ; CW-HW
    9     10    1    0.1080    284512.0 ; CM-HM
    9     11    1    0.1080    284512.0 ; CM-HM
    9     12    1    0.1080    284512.0 ; CM-HM
    13    14    1    0.1080    284512.0 ; CA-HA
    13    15    1    0.1080    284512.0 ; CA-HA
    13    16    1    0.1526    224262.4 ; CA-CS
    16    17    1    0.1087    284512.0 ; CS-HS
    16    18    1    0.1087    284512.0 ; CS-HS
    16    19    1    0.1531    224262.4 ; CS-CS
    19    20    1    0.1087    284512.0 ; CS-HS
    19    21    1    0.1087    284512.0 ; CS-HS
    19    22    1    0.1528    224262.4 ; CS-CT
    22    23    1    0.1084    284512.0 ; CT-HT
    22    24    1    0.1084    284512.0 ; CT-HT
    22    25    1    0.1084    284512.0 ; CT-HT

    [  angles  ]
;   ai    aj    ak funct  c0(deg)   c1(kJ mol-1 rad-2)
    1     3     2    1    109.80    585.76 ; NA-CR-NA
    1     3     4    1    125.10    292.88 ; NA-CR-HR
    1     5     6    1    122.00    292.88 ; NA-CW-HW
    1     5     7    1    107.10    585.76 ; NA-CW-CW
    1     13    14   1    107.50    313.80 ; NA-CA-HA
    1     13    15   1    107.50    313.80 ; NA-CA-HA
    1     13    16   1    113.00    488.27 ; NA-CA-CS
```

```
    2     3     4    1    125.10    292.88 ; NA-CR-HR
    2     7     5    1    107.10    585.76 ; NA-CW-CW
    2     7     8    1    122.00    292.88 ; NA-CW-HW
    2     9    10    1    109.20    313.80 ; NA-CM-HM
    2     9    11    1    109.20    313.80 ; NA-CM-HM
    2     9    12    1    109.20    313.80 ; NA-CM-HM
    5     1     3    1    107.90    585.76 ; CW-NA-CR
    5     7     8    1    130.90    292.88 ; CW-CW-HW
    7     2     3    1    107.90    585.76 ; CW-NA-CR
    7     5     6    1    130.90    292.88 ; CW-CW-HW
    9     2     3    1    126.40    585.76 ; CM-NA-CR
    9     2     7    1    125.60    585.76 ; CM-NA-CW
   11     9    10    1    109.80    276.14 ; HM-CM-HM
   12     9    10    1    109.80    276.14 ; HM-CM-HM
   12     9    11    1    109.80    276.14 ; HM-CM-HM
   13     1     3    1    126.80    585.76 ; CA-NA-CR
   13     1     5    1    125.30    585.76 ; CA-NA-CW
   13    16    17    1    108.60    313.80 ; CA-CS-HS
   13    16    18    1    108.60    313.80 ; CA-CS-HS
   13    16    19    1    113.30    488.27 ; CA-CS-CS
   14    13    15    1    108.90    276.14 ; HA-CA-HA
   14    13    16    1    111.10    313.80 ; HA-CA-CS
   15    13    16    1    111.10    313.80 ; HA-CA-CS
   16    19    20    1    109.60    313.80 ; CS-CS-HS
   16    19    21    1    109.60    313.80 ; CS-CS-HS
   16    19    22    1    112.30    488.27 ; CS-CS-CT
   17    16    18    1    106.70    276.14 ; HS-CS-HS
   19    16    17    1    109.60    313.80 ; CS-CS-HS
   19    16    18    1    109.60    313.80 ; CS-CS-HS
   19    22    23    1    111.10    313.80 ; CS-CT-HT
   19    22    24    1    111.10    313.80 ; CS-CT-HT
   19    22    25    1    111.10    313.80 ; CS-CT-HT
   21    19    20    1    106.70    276.14 ; HS-CS-HS
   22    19    20    1    109.70    313.80 ; CT-CS-HS
   22    19    21    1    109.70    313.80 ; CT-CS-HS
   24    22    23    1    107.90    276.14 ; HT-CT-HT
   25    22    23    1    107.90    276.14 ; HT-CT-HT
   25    22    24    1    107.90    276.14 ; HT-CT-HT

   [  dihedrals  ]
;   ai    aj    ak    al funct    c0        c1      c2     c3(kJ/mol)
    1     5     7     2     5    0.000    44.980   0.000    0.000 ; NA-CW-CW-NA
    1     5     7     8     5    0.000    44.980   0.000    0.000 ; NA-CW-CW-HW
    1    13    16    17     5    0.000    0.000    0.000    0.000 ; NA-CA-CS-HS
    1    13    16    18     5    0.000    0.000    0.000    0.000 ; NA-CA-CS-HS
    1    13    16    19     5   -3.297    3.347    1.674    0.000 ; NA-CA-CS-CS
    3     1     5     6     5    0.000    12.552   0.000    0.000 ; CR-NA-CW-HW
    3     1     5     7     5    0.000    12.552   0.000    0.000 ; CR-NA-CW-CW
    3     1    13    14     5    0.000    0.000    0.000    0.000 ; CR-NA-CA-HA
    3     1    13    15     5    0.000    0.000    0.000    0.000 ; CR-NA-CA-HA
    3     1    13    16     5   -0.665    0.397   -0.042    0.000 ; CR-NA-CA-CS
    3     2     7     5     5    0.000    12.552   0.000    0.000 ; CR-NA-CW-CW
    3     2     7     8     5    0.000    12.552   0.000    0.000 ; CR-NA-CW-HW
    3     2     9    10     5    0.000    0.000    0.000    0.000 ; CR-NA-CM-HM
    3     2     9    11     5    0.000    0.000    0.000    0.000 ; CR-NA-CM-HM
    3     2     9    12     5    0.000    0.000    0.000    0.000 ; CR-NA-CM-HM
    5     1     3     2     5    0.000    19.460   0.000    0.000 ; CW-NA-CR-NA
    5     1     3     4     5    0.000    19.460   0.000    0.000 ; CW-NA-CR-HR
    5     1    13    14     5   -11.297  -23.640   1.485    0.000 ; CW-NA-CA-HA
    5     1    13    15     5   -11.297  -23.640   1.485    0.000 ; CW-NA-CA-HA
    5     1    13    16     5   -8.828   -20.920   1.443    0.000 ; CW-NA-CA-CS
    6     5     7     2     5    0.000    44.978   0.000    0.000 ; HW-CW-CW-NA
    6     5     7     8     5    0.000    44.978   0.000    0.000 ; HW-CW-CW-HW
    7     2     3     1     5    0.000    19.460   0.000    0.000 ; CW-NA-CR-NA
    7     2     3     4     5    0.000    19.460   0.000    0.000 ; CW-NA-CR-HR
    7     2     9    10     5    0.000    0.000    0.519    0.000 ; CW-NA-CM-HM
    7     2     9    11     5    0.000    0.000    0.519    0.000 ; CW-NA-CM-HM
    7     2     9    12     5    0.000    0.000    0.519    0.000 ; CW-NA-CM-HM
    9     2     3     1     5    0.000    19.460   0.000    0.000 ; CM-NA-CR-NA
    9     2     3     4     5    0.000    19.460   0.000    0.000 ; CM-NA-CR-HR
    9     2     7     5     5    0.000    12.552   0.000    0.000 ; CM-NA-CW-CW
```

```
     9     2     7     8     5     0.000    12.552    0.000    0.000 ; CM-NA-CW-HW
     13    1     3     2     5     0.000    19.460    0.000    0.000 ; CA-NA-CR-NA
     13    1     3     4     5     0.000    19.460    0.000    0.000 ; CA-NA-CR-HR
     13    1     5     6     5     0.000    12.552    0.000    0.000 ; CA-NA-CW-HW
     13    1     5     7     5     0.000    12.552    0.000    0.000 ; CA-NA-CW-CW
     13    16    19    20    5     0.000     0.000    1.531    0.000 ; CA-CS-CS-HS
     13    16    19    21    5     0.000     0.000    1.531    0.000 ; CA-CS-CS-HS
     13    16    19    22    5     5.439    -0.209    0.837    0.000 ; CA-CS-CS-CT
     14    13    16    17    5     0.000    -0.628    2.167    0.000 ; HA-CA-CS-HS
     14    13    16    18    5     0.000    -0.628    2.167    0.000 ; HA-CA-CS-HS
     14    13    16    19    5     0.000     0.000    1.531    0.000 ; HA-CA-CS-CS
     15    13    16    17    5     0.000    -0.628    2.167    0.000 ; HA-CA-CS-HS
     15    13    16    18    5     0.000    -0.628    2.167    0.000 ; HA-CA-CS-HS
     15    13    16    19    5     0.000     0.000    1.531    0.000 ; HA-CA-CS-CS
     16    19    22    23    5     0.000     0.000    1.531    0.000 ; CS-CS-CT-HT
     16    19    22    24    5     0.000     0.000    1.531    0.000 ; CS-CS-CT-HT
     16    19    22    25    5     0.000     0.000    1.531    0.000 ; CS-CS-CT-HT
     17    16    19    20    5     0.000     0.000    1.331    0.000 ; HS-CS-CS-HS
     17    16    19    21    5     0.000     0.000    1.331    0.000 ; HS-CS-CS-HS
     17    16    19    22    5     0.000     0.000    1.531    0.000 ; HS-CS-CS-CT
     18    16    19    20    5     0.000     0.000    1.331    0.000 ; HS-CS-CS-HS
     18    16    19    21    5     0.000     0.000    1.331    0.000 ; HS-CS-CS-HS
     18    16    19    22    5     0.000     0.000    1.531    0.000 ; HS-CS-CS-CT
     20    19    22    23    5     0.000     0.000    1.331    0.000 ; HS-CS-CT-HT
     20    19    22    24    5     0.000     0.000    1.331    0.000 ; HS-CS-CT-HT
     20    19    22    25    5     0.000     0.000    1.331    0.000 ; HS-CS-CT-HT
     21    19    22    23    5     0.000     0.000    1.331    0.000 ; HS-CS-CT-HT
     21    19    22    24    5     0.000     0.000    1.331    0.000 ; HS-CS-CT-HT
     21    19    22    25    5     0.000     0.000    1.331    0.000 ; HS-CS-CT-HT
     9     2     3     7     5     0.000     8.368    0.000    0.000 ; CM-NA-CR-CW  improper
     13    1     3     5     5     0.000     8.368    0.000    0.000 ; CA-NA-CR-CW  improper
     6     5     1     7     5     0.000     9.205    0.000    0.000 ; HW-CW-NA-CW  improper
     8     7     2     5     5     0.000     9.205    0.000    0.000 ; HW-CW-NA-CW  improper
     4     3     2     1     5     0.000     9.205    0.000    0.000 ; HR-CR-NA-NA  improper
```

Table S6. Bonded parameters for the anion, $[PF_6]^-$, `PF6.itp` file.

```
    [  moleculetype  ]
;   name    nrexcl
    PF6    3

    [  atoms  ]
;   nr type resnr residu atom cgnr  charge     mass
    1    P    1    PF6    P1    1     1.072    30.974
    2    F    1    PF6    F2    1    -0.312    18.998
    3    F    1    PF6    F3    1    -0.312    18.998
    4    F    1    PF6    F4    1    -0.312    18.998
    5    F    1    PF6    F5    1    -0.312    18.998
    6    F    1    PF6    F6    1    -0.312    18.998
    7    F    1    PF6    F7    1    -0.312    18.998

    [  bonds  ]
;   ai   aj funct  c0(nm)   c1(kJ mol-1 nm-2)
    1    2    1    0.1606    310000    ; P-F
    1    3    1    0.1606    310000    ; P-F
    1    4    1    0.1606    310000    ; P-F
    1    5    1    0.1606    310000    ; P-F
    1    6    1    0.1606    310000    ; P-F
    1    7    1    0.1606    310000    ; P-F

    [  angles  ]
;   ai   aj   ak funct c0(deg) c1(kJ mol-1 rad-2)
    2    1    3    1    90    1165    ; F-P-F
    2    1    4    1    90    1165    ; F-P-F
    2    1    6    1    90    1165    ; F-P-F
    2    1    7    1    90    1165    ; F-P-F
    3    1    4    1    90    1165    ; F-P-F
    3    1    5    1    90    1165    ; F-P-F
    3    1    7    1    90    1165    ; F-P-F
    4    1    5    1    90    1165    ; F-P-F
    4    1    6    1    90    1165    ; F-P-F
    5    1    6    1    90    1165    ; F-P-F
    5    1    7    1    90    1165    ; F-P-F
    6    1    7    1    90    1165    ; F-P-F
```

Table S7. Bonded parameters for CO_2, `CO2.itp` file.

```
    [  moleculetype  ]
;   name   nrexcl
    CO2    2

    [  atoms  ]
;   nr type resnr residu atom cgnr   charge    mass
    1     O     1    CO2   O1    1   -0.350    15.99940
    2     C     1    CO2   C1    1    0.700    12.01070
    3     O     1    CO2   O2    1   -0.350    15.99940

    [  bonds  ]
;   ai   aj funct   c0(nm)   c1(kJ mol-1 nm-2)
    1    2    1     0.1160   861070
    2    3    1     0.1160   861070

    [  angles  ]
;   ai   aj   ak funct   c0(deg)   c1(kJ mol-1 rad-2)
    1    2    3      1   180       468.61
```

Table S8. Bonded parameters for N_2, `N2.itp` file.

```
    [  moleculetype  ]
;  name   nrexcl
     N2        2

    [  atoms  ]
;  nr type resnr residu atom cgnr   charge    mass
    1    N     1     N2   N1    1   -0.482    14.00670
    2    N     1     N2   N2    1   -0.482    14.00670
    3   MW     1     N2  MW1    1    0.964    0.000000

    [ constraints ]
;  ai   aj funct    c0(nm)
    1    2     1    0.110

    [ exclusions ]
;  ai   aj   ak
    1    2    3
    2    1    3
    3    1    2

    [ virtual_sites2 ]
;  ai   aj   ak funct   a
    3    1    2     1   0.5
```

5. ITIM parameters

Here we describe some details on calculating intrinsic density profiles of atoms using the ITIM methodology. Files required to carry out these calculations are provided, see the link

https://github.com/SarkisovGroup/Interfaces.git

The ITIM code carries out an intrinsic analysis of macroscopically planar liquid-liquid interfaces. It uses the ITIM method[7] to find the true set of interfacial sites, then applies triangular interpolation[8,9] to approximate the surface for the calculation of intrinsic profiles. It is assumed that the *z*-coordinate is normal to the interfacial plane.

1 step – compilation of files (folder "ITIM_code").

```
c++ itim5.C -o itim5
```

2 step – calculation of density profiles (folder with a trajectory file, `traj_comp.xtc`).

The code can be run starting from an input data file with atomic coordinates or directly from the MD trajectory, as follows:

```
gmx_mpi dump -f traj_comp.xtc | ./xtc.pl n_molecules_of_sp1 n_sites_of_sp1
n_molecules_of_sp2 n_sites_of_sp2 | ./itim5 - param_file nsteps
```

Example of calculation of intrinsic density profiles of atoms over a whole trajectory for a system containing 500 ion pairs, 100 molecules of CO_2 and N_2 each:

```
gmx_mpi dump -f traj_comp.xtc | ./xtc.pl 500 25 500 7 100 3 100 3 | ./itim5 - param.inp
```

The simulation may contain any number of different species. Each species contains a given number of molecules, each composed of a given number of sites. For the analysis, the system is divided into two distinct phases, and each species is assigned to a given phase. Only two phases can be used in this version of the program. The set of interfacial molecules is then searched in the entire phase, while profiles are calculated separately for each species.

The file `xtc.pl` is a script to convert the Gromacs trajectory to an appropriate format used by the code. Depending on the number of species, the following part of the `xtc.pl` file should be edited. For example the following part of the script says to report molecules of species 1 (`$nSp1Mols.`) in phase 1 (`"\n"`) but not in phase 2 (`"0\n"`). The same applies to species 2. Species 1 and 2 are $[BMIM]^+$ and $[PF_6]^-$ respectively. Species 3 and 4 that are CO_2 and N_2 are not reported in phase 1 but reported in phase 2. Thus, the sequence is as shown below.

```
        print $nSp1Mols."\n"; BMIM in Phase 1

    for ($i=0; $i<$nAtoms;  $i++) {
        if ($i==$nSp1Mols*$nSp1Sites) {
            print "0 \n"; BMIM not in Phase 2
            print $nSp2Mols."\n"; PF6 in Phase 1
        }

        if ($i==($nSp1Mols*$nSp1Sites+$nSp2Mols*$nSp2Sites)) {
            print "0 \n"; PF6 not in Phase 2
            print "0 \n"; CO2 not in Phase 1
            print $nSp3Mols."\n"; CO2 in Phase 2
        }
        if ($i==($nSp1Mols*$nSp1Sites+$nSp2Mols*$nSp2Sites+$nSp3Mols*$nSp3Sites)) {
            print "0 \n"; N2 not in Phase 1
```

```
            print $nSp4Mols."\n"; N2 in Phase 2
```

Input parameters for calculation of density profiles are provided in `param.inp` file which has a specific format shown below.

```
464
4

112
0.2
112
0.125

500
25
14.007  0.176 0.325   0.711280 1
14.007  0.176 0.325   0.711280 1
12.011 -0.072 0.355   0.292880 1
 1.008  0.168 0.242   0.125520 1
12.011 -0.192 0.355   0.292880 1
 1.008  0.216 0.242   0.125520 1
12.011 -0.192 0.355   0.292880 1
 1.008  0.216 0.242   0.125520 1
12.011 -0.280 0.350   0.276144 1
 1.008  0.144 0.250   0.125520 1
 1.008  0.144 0.250   0.125520 1
 1.008  0.144 0.250   0.125520 1
12.011 -0.136 0.350   0.276144 1
 1.008  0.144 0.250   0.125520 1
 1.008  0.144 0.250   0.125520 1
12.011 -0.096 0.350   0.276144 1
 1.008  0.048 0.250   0.125520 1
 1.008  0.048 0.250   0.125520 1
12.011 -0.096 0.350   0.276144 1
 1.008  0.048 0.250   0.125520 1
 1.008  0.048 0.250   0.125520 1
12.011 -0.192 0.350   0.276144 1
 1.008  0.064 0.250   0.125520 1
 1.008  0.064 0.250   0.125520 1
 1.008  0.064 0.250   0.125520 1

500
7
30.974  1.072 0.37400 0.83700  1
18.998 -0.312 0.31181 0.25522  1
18.998 -0.312 0.31181 0.25522  1
18.998 -0.312 0.31181 0.25522  1
18.998 -0.312 0.31181 0.25522  1
18.998 -0.312 0.31181 0.25522  1
18.998 -0.312 0.31181 0.25522  1

100
3
12.01070 -0.350 0.305 0.656842 1
15.99940  0.700 0.280 0.224490 1
12.01070 -0.350 0.305 0.656842 1

100
3
14.0067  -0.482 0.331 0.299214 1
14.0067  -0.482 0.331 0.299214 1
0.00000   0.964 0.000 0.000000 0
```

The first 2 lines correspond to general information where *464* is the number of slabs in the *z*-direction of the simulation box (L_Z, *nm*) for the calculation of density profiles and is equal to L_Z / *0.04*, where *0.04 nm* is the optimum spacing; *4* is the total number of species in the system (this must match the number of species in the MD trajectory): $[BMIM]^+$, $[PF_6]^-$, CO_2, N_2 (see `*.top` file).

The next 4 lines correspond to ITIM or interface parameters where *112* is the number of test lines (grid in *x*-, *y*-direction of the simulation box) of the ITIM method for phase *1* which is positioned at the center of the box and is equal to L_X */ 0.05* and L_Y */ 0.05*, where *0.05 nm* is the optimum spacing; *0.2* is the probe sphere radius of the ITIM method for phase *1*; *0.125* is the probe sphere radius of the ITIM method for phase *2*.

Next, data for each species is provided. In this particular example, there are 4 species ($[BMIM]^+$, $[PF_6]^-$, CO_2, N_2) and, therefore, 4 blocks. For the first block, corresponding to $[BMIM]^+$, *500* is the total number of molecules (ions) of species *1* (for example, 500 ions of $[BMIM]^+$); *25* is the number of sites (atoms) for each molecule (ion) of species *1* (for example, 25 atoms in $[BMIM]^+$). Five columns correspond to parameters for each site: mass (g/mol), charge (*a.u.*), σ (*nm*), ε (*kJ/mol*), and "profile" (*0* or *1*). A site with σ = *0.0* is not included in the search for interfacial sites. Variable "profile" (*0* or *1*) determines if a density profile is (*1*) or not (*0*) calculated for this site.

6. Analytical procedure and mathematical criteria used to investigate gas density profiles

In Figure S1, we show how to split gas density profiles into three parts: the gas amount absorbed in the bulk ionic liquid phase, the excess amount adsorbed on the surface and the bulk gas phase. First, we identify the position of the ITIM surface (IS) using the density profile of the ionic liquid (not shown here). Then, starting from the center of the film we smooth the gas density profile over all data points (red curve) moving towards the IS. Next, we fit an exponential function (blue curve) to the left half of the main peak of the gas density profile. The intersection point of these two curves defines the constant density value of the gas dissolved in the ionic liquid (red area). The estimated CO_2 solubility includes a contribution from gas molecules that accumulate between the surface and the sub-surface layers of the ionic liquid (Figure S1(a) and Figure 8(a)). For nitrogen, blue and red curves may not intercept because nitrogen solubility in the ionic liquid is low. In this case, we find the intercept between black and blue curves and extrapolate a perpendicular line (dash line in Figure S1(b), inset) from the intercept towards the red curve where a new intercept point determines the density of the gas dissolved in the liquid phase. The red area extends towards the ITIM surface (IS). The blue area which corresponds to the amount of gas present in the bulk gas phase is calculated by averaging the bulk gas density and also extending it towards the IS. For low-pressure systems (large simulation box) density profiles of the bulk gas are not uniform. To find the right boundary between the excess (yellow area) and bulk (blue area) amounts of gas, we averaged the bulk gas profile over a 5-10 nm region and extended the blue area towards the IS, and, then, took 99.73 % of the total yellow area of the right half of the peak. This value of the integrated yellow area falls within 3 standard deviations of the mean according to the Gaussian distribution. The total blue area is calculated as the summation of the blue area extended towards the IS and the integrated area below the density profile. After accounting for the absorbed and bulk gas, the remainder is the excess amount of gas represented by the yellow area.

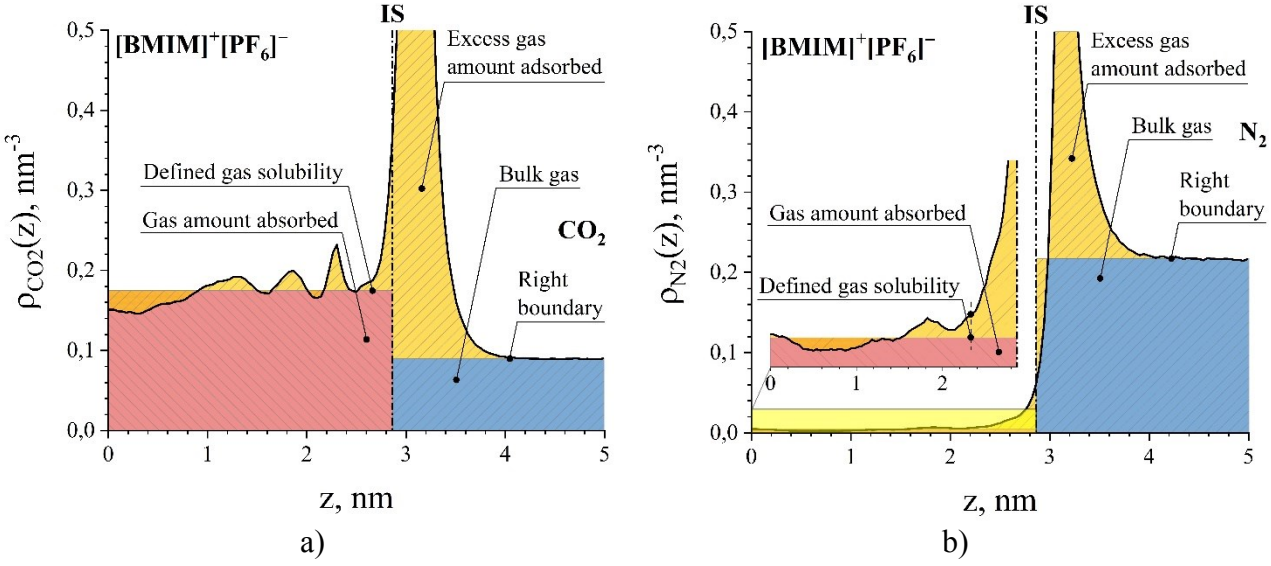

Figure S1. Identification of different regions of the gas density profiles for a) – carbon dioxide and b) – nitrogen interacting with the film of ionic liquid, $[BMIM]^+[PF_6]^-$. IS is the ITIM surface. The black curve is the gas density profile; the red curve is the average gas density profile obtained using a cumulative moving average technique; the blue curve is a fitted exponential function to the left half of the main peak. The inset shows a more detailed picture within the yellow-shaded area. For the purpose of illustration, the profiles here correspond to the conditions of system 12 in Table 1.

The same procedure is used to estimate the excess amount of gas from global density profiles with the only exception that the definition of the Gibbs dividing surface should be used instead of the ITIM surface.

7. Full derivations of equations presented in the main text of the paper

Equation (8).

We begin our derivation of equation (8) from the definition of Henry's constant. The amount of gas dissolved in the bulk liquid and adsorbed on the surface is expressed as:

$$\rho = \frac{N_{i,\rho}}{V} = \frac{P_i}{H_{i,\rho}} \tag{S3}$$

$$\sigma = \frac{N_{i,\sigma}}{S} = \frac{P_i}{H_{i,\sigma}} \tag{S4}$$

where ρ is the number density of gas in the bulk volume of ionic liquid, nm^{-3}; σ is the excess number density of gas on the surface of ionic liquid, nm^{-2}; N_ρ and N_σ represent the amount of gas component i absorbed in and adsorbed on a film of ionic liquid; V (nm^3) and S (nm^2) are the volume and the surface area of the liquid phase respectively; H_ρ ($MPa \cdot nm^3$) and H_σ ($MPa \cdot nm^2$) are the Henry's constants describing solubility and adsorption of gas component i at low partial pressure P (MPa).

Using the definition of the equipartition thickness (equation (7)) and assuming the Henry's law regime of gas adsorption and absorption (equations (S3) and (S4)), we obtain:

$$h_{eq}(P) = \frac{\sigma}{\rho} = \frac{P_i \cdot H_{i,\rho}}{H_{i,\sigma} \cdot P_i} = \frac{H_{i,\rho}}{H_{i,\sigma}} \tag{S5}$$

Equation (9).

In order to derive equation (9) we use a standard definition of gas selectivity for the bulk and interfacial regions of a film of ionic liquid, consider the bulk gas phase as the ideal gas, and assume the Henry's law regime of gas adsorption on and absorption in a thin film of ionic liquid.

$$S_{i,j,\rho} = \frac{N_{i,\rho}/N_{i,\gamma}}{N_{j,\rho}/N_{j,\gamma}} = \frac{N_{i,\rho}/(P_i \cdot V)}{N_{j,\rho}/(P_j \cdot V)} = \frac{H_{j,\rho}}{H_{i,\rho}} \tag{S6}$$

where $S_{i,j,\rho}$ is the selectivity of the bulk (ρ) region of a film of ionic liquid with respect to species i and j; N_γ represent the bulk amount of gas species i and j.

The analogous expression is used to calculate the gas selectivity of the surface of the thin film of ionic liquids. Using equations (8) and (S6) we derive equation (9) which relates the equipartition thicknesses (h_{eq}, nm) for gas components i and j and selectivities of the bulk and interfacial regions of the thin film of an ionic liquid.

$$\frac{h_{eq}^{\,i}}{h_{eq}^{\,j}} = \frac{H_{i,\rho}}{H_{i,\sigma}} \cdot \frac{H_{j,\sigma}}{H_{j,\rho}} = \frac{H_{i,\rho}}{H_{j,\rho}} \cdot \frac{H_{j,\sigma}}{H_{i,\sigma}} = \frac{S_{i,j,\sigma}}{S_{i,j,\rho}} \tag{S7}$$

Equation (11).

First, we define the total selectivity of the film of an ionic liquid:

$$S_{i,j} = \frac{(N_{i,\rho} + N_{i,\sigma})/N_{i,\gamma}}{(N_{j,\rho} + N_{j,\sigma})/N_{j,\gamma}} \tag{S8}$$

Next, we use the ideal gas equation of state to express N_γ through partial pressures of gas components *i* and *j* and substitute equations (S3) and (S4) for gas components *i* and *j* into equation (S8), thus deriving equation (11):

$$S_{i,j}(h) = \frac{\left(\frac{P_i \cdot S \cdot h}{H_{i,\rho}} + \frac{P_i \cdot S}{H_{i,\sigma}}\right)\Big/\frac{P_i V}{RT}}{\left(\frac{P_j \cdot S \cdot h}{H_{j,\rho}} + \frac{P_j \cdot S}{H_{j,\sigma}}\right)\Big/\frac{P_j V}{RT}} = \frac{\frac{h}{H_{i,\rho}} + \frac{1}{H_{i,\sigma}}}{\frac{h}{H_{j,\rho}} + \frac{1}{H_{j,\sigma}}} = \tag{S9}$$

$$= \frac{H_{j,\rho} \cdot H_{j,\sigma}}{H_{i,\rho} \cdot H_{i,\sigma}} \cdot \frac{H_{i,\sigma} \cdot h + H_{i,\rho}}{H_{j,\sigma} \cdot h + H_{j,\rho}} = S_{i,j,\rho} \cdot S_{i,j,\sigma} \cdot \left[\frac{H_{i,\sigma} \cdot h + H_{i,\rho}}{H_{j,\sigma} \cdot h + H_{j,\rho}}\right]$$

where *h* is the thickness of a film of ionic liquid, *nm*; *R* is the universal gas constant; *T* is the temperature, *K*, and all other terms are defined as before.

Equations (14) and (15).

Using equations (12) for gas absorption in the ionic liquid and adsorption on the surface of the film we derive equation (14).

$$\left(\frac{\partial ln(H_\rho)}{\partial(1/T)}\right)_P = \left(\frac{\Delta\bar{h}_\rho}{R}\right) \tag{S10}$$

subtract

$$\left(\frac{\partial ln(H_\sigma)}{\partial(1/T)}\right)_P = \left(\frac{\Delta\bar{h}_\sigma}{R}\right) \tag{S11}$$

where $\Delta\bar{h}_\rho$ and $\Delta\bar{h}_\sigma$ are the are the partial molar change of enthalpy of absorption and adsorption, respectively, *J/mol*.

Then, substitute equation (8) into the obtained relation (S12)

$$\left(\frac{\partial ln(\frac{H_\rho}{H_\sigma})}{\partial(1/T)}\right)_P = \left(\frac{\Delta\bar{h}_\rho - \Delta\bar{h}_\sigma}{R}\right) \tag{S12}$$

$$\left(\frac{\partial ln(h_{eq})}{\partial(1/T)}\right)_P = \left(\frac{\Delta\bar{h}_\rho - \Delta\bar{h}_\sigma}{R}\right)$$

The same procedure is used to derive equation (15) starting from equation (13).

8. Gas absorption and excess adsorption isotherms at 323.15, 343.15, and 393.15 K

In this section, we present a full set of isotherms describing CO_2 and N_2 adsorption and absorption from binary and ternary mixtures of ionic liquid and gas. The presented isotherms in Figure S2 are obtained from MD simulations for systems listed in Table S1. All data points in Figures S2(a, b, c) are fitted with the Henry's law models while data points in Figure S2(d) are fitted with and the Langmuir model.

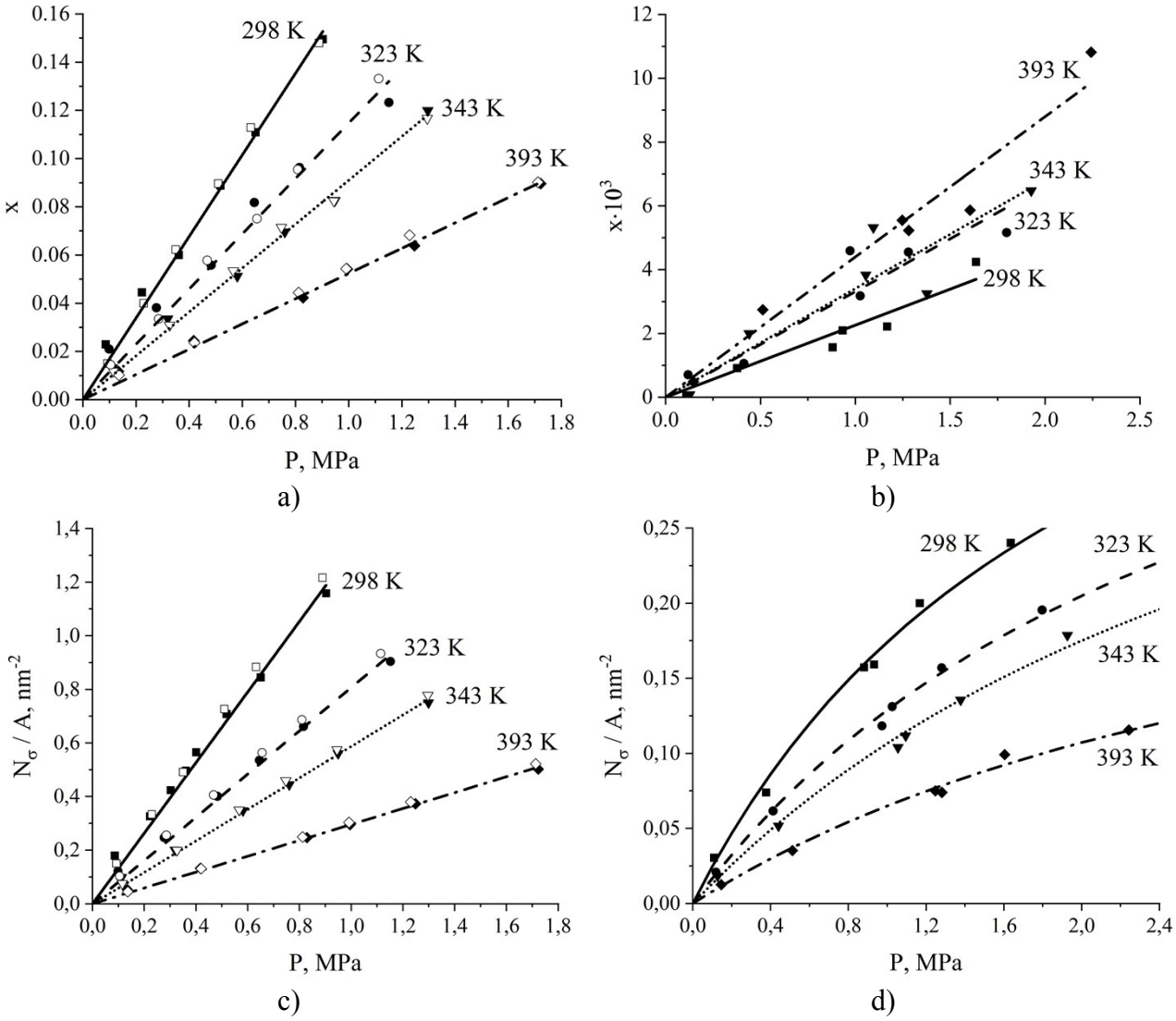

Figure S2. Gas absorption and excess adsorption per surface area of ionic liquid film isotherms for carbon dioxide (a, c) and nitrogen (b, d) dissolved in the ionic liquid, $[BMIM]^+[PF_6]^-$. MD simulations were carried out for binary (open symbols) and ternary (filled symbols) mixtures of ionic liquid and gas, where gas is present as a mixture of carbon dioxide and nitrogen or a single component of either carbon dioxide or nitrogen. The black lines in a), b) and c) are the Henry's law models and in d) the Langmuir models fitted to the simulation data for ternary mixtures.

Figure S3 shows experimental and simulation results for CO_2 solubility in terms of mole fraction (Figure S3(a)) and the Henry's constants (Figure S3(b)) as a function of temperature.

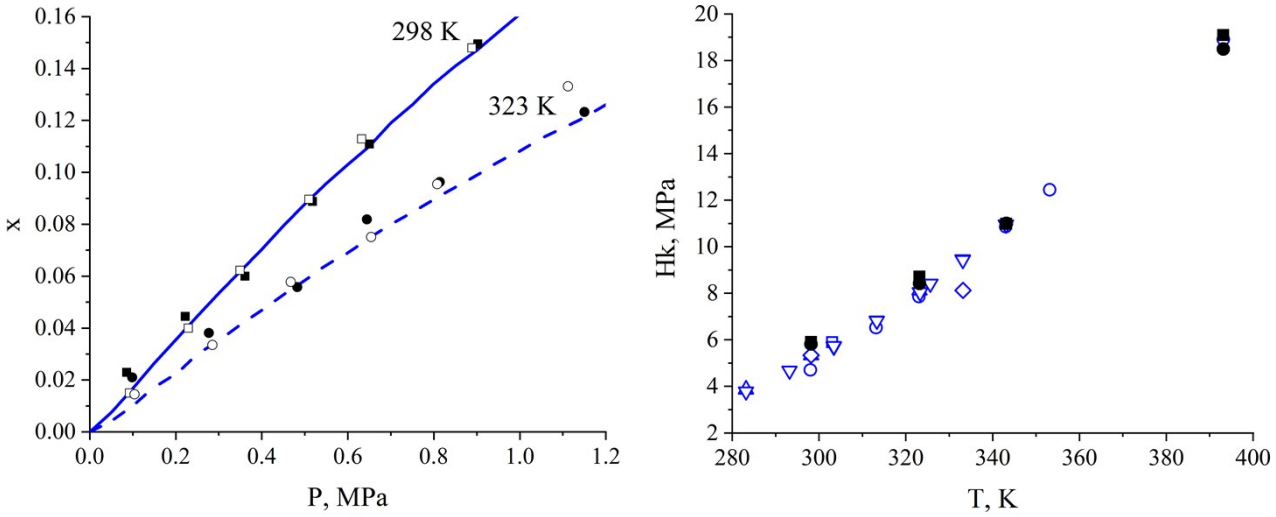

Figure S3. (a) – Absorption isotherms for carbon dioxide dissolved in the ionic liquid, $[BMIM]^+[PF_6]^-$. The blue curves are experimental data reproduced from.[10] Points were obtained from MD simulations of binary (open symbols) and ternary (filled symbols) mixtures of ionic liquid and gas, where gas is present as a mixture of carbon dioxide and nitrogen or a single component of either carbon dioxide or nitrogen. (b) – the Henry's constants for carbon dioxide dissolved in the ionic liquid, $[BMIM]^+[PF_6]^-$ as a function of temperature. Open symbols are experimental data reproduced from corresponding literature: up triangle[10], square[11], circle[12], down triangle[13], diamond[14]. Filled symbols are data points obtained from MD simulation of binary (circle) and ternary (square) mixtures of ionic liquid and gas, where gas is present as a mixture of carbon dioxide and nitrogen or a single component of either carbon dioxide or nitrogen.

We use the Peng-Robinson equation of state[15] for calculating partial pressures of each gas component where gas density and volume correspond to the bulk gas region. In their original work, Peng and Robinson correctly predicted experimental vapor pressure for CO_2 and N_2 using the proposed equation of state. In addition, Potoff and Siepmann showed that CO_2 and N_2 TraPPE models were able to carefully reproduce experimental phase equilibrium properties of real gases over a broad range of temperatures and pressures.[16] In a comprehensive comparison of different CO_2 force fields, Aimoli et al. showed that the TraPPE model and the Peng-Robinson equation of state correctly reproduce thermodynamic properties from experiments at pressure and temperature of interest.[17] Thus, this allows us to use the Peng-Robinson equation of state to describe gas pressure in the simulated systems.

9. Equipartition thickness for carbon dioxide and nitrogen

Figure S4 shows that the equipartition thickness for carbon dioxide is independent of pressure at elevated temperatures. In particular, we obtain h_{eq} equal to 2.4 nm at 323 K, 2.2 nm at 343 K, and 2.1 nm at 393 K using equation (8). For nitrogen, using equation (7) we observe that the equipartition thickness deviates from the Henry's law regime of adsorption. For the Henry's law region h_{eq} with respect to nitrogen is equal to 19 nm at 323 K, 14 nm at 343 K, and 7.2 nm at 393 K calculated from equation (8).

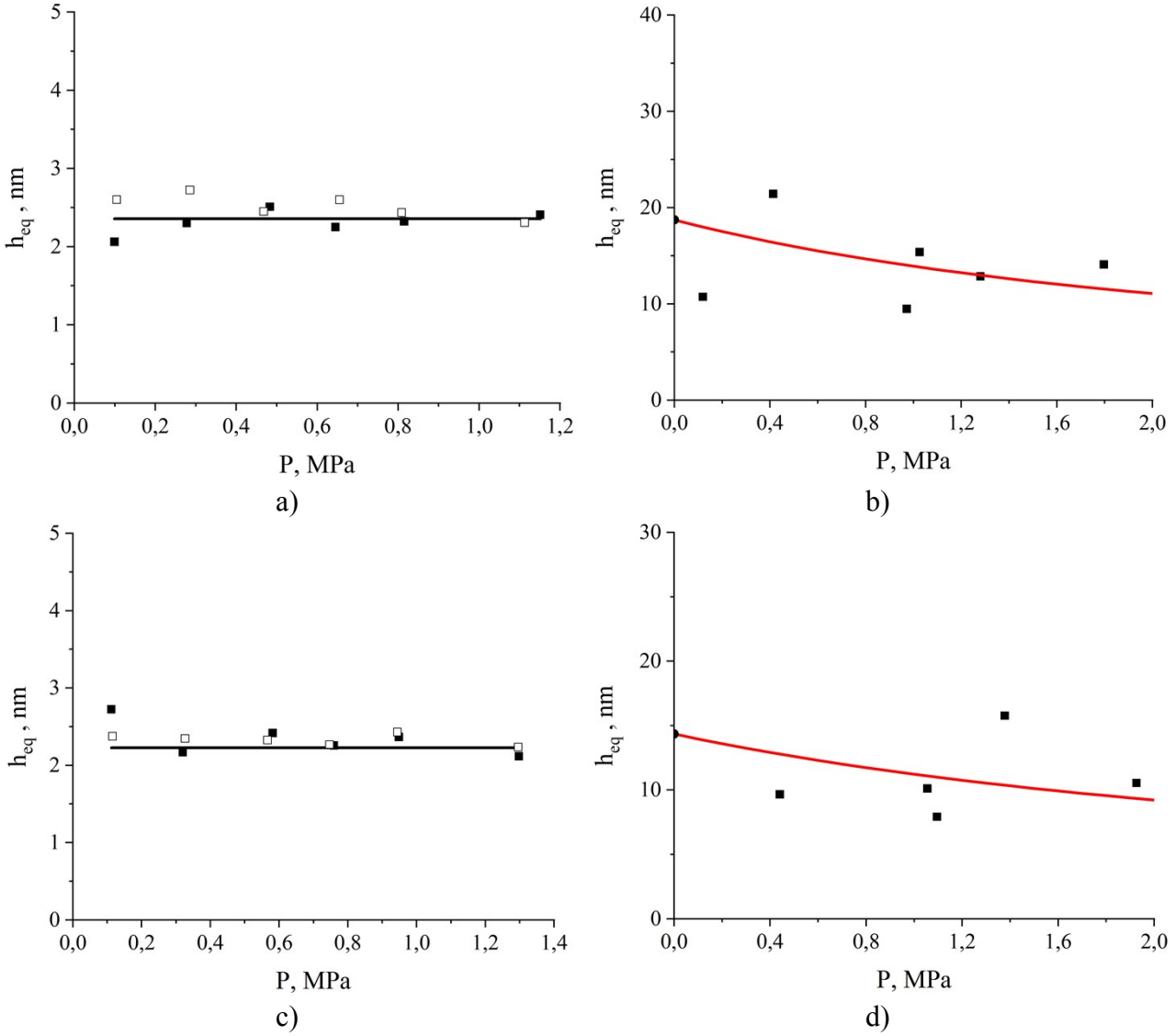

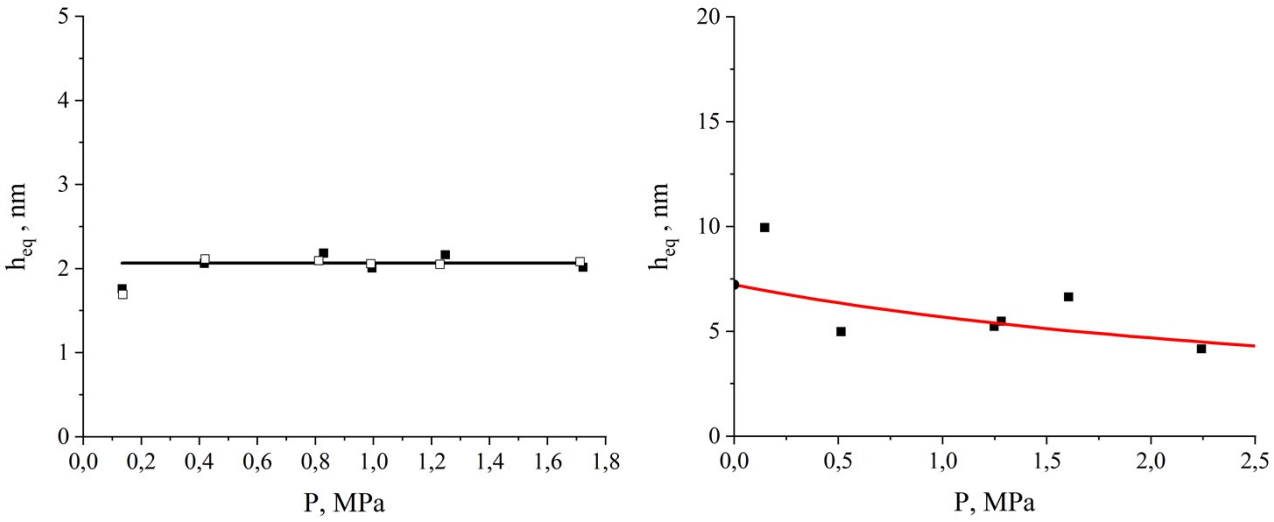

Figure S4. The equipartition thickness as a function of partial pressure at 323 K (a, b), 343 K (c, d), 393 K (e, f): left column – CO_2, right column – N_2. The simulated system contains ionic liquid, $[BMIM]^+[PF_6]^-$, exposed to the corresponding single gas component (open square symbols) or a mixture of CO_2 and N_2 (filled square symbols); the black solid line and the black filled circle at P = 0 MPa for the left column are the values calculated according to equation (8); the red curve is calculated according to equation (7) using the Langmuir model for N_2 adsorption.

Figure S5 shows that $ln(h_{eq})$ is linearly proportional to $1/T$ and $ln(T)$, therefore, $\Delta\bar{h}_\rho - \Delta\bar{h}_\sigma$ and $\Delta\bar{s}_\sigma - \Delta\bar{s}_\rho$ are independent of temperature. We fit linear functions to both sets of data for CO_2 and N_2 adsorption assuming that adsorption from the gas phase obeys the Henry's law.

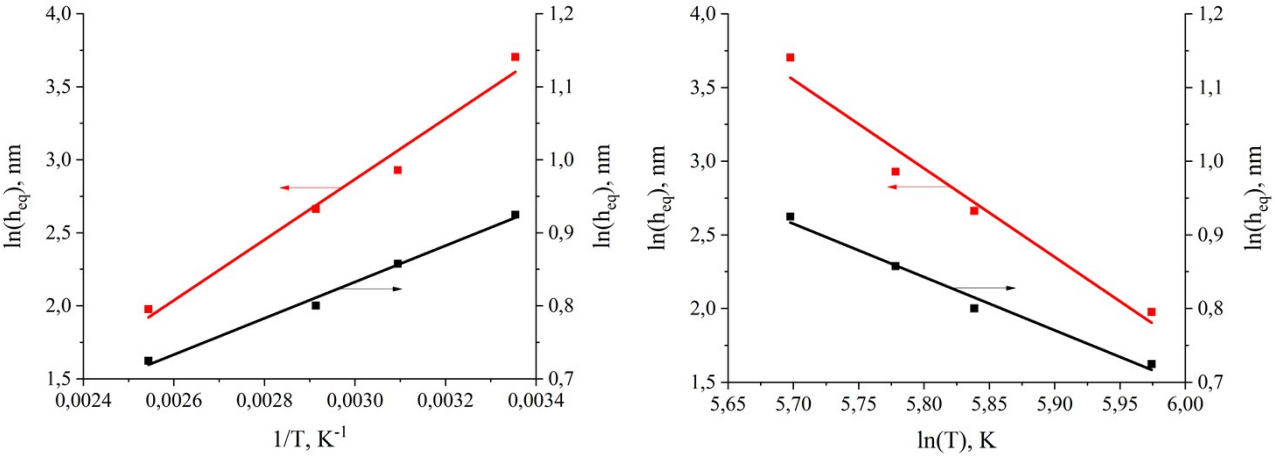

Figure S5. The equipartition thickness for CO_2 (black line and symbols) and N_2 (red line and symbols) adsorption from a single (open symbols) and a two-component (CO_2 and N_2) (filled symbols) gas phase.

10. Key properties characterizing gas adsorption and absorption in thin films of ionic liquid

Table S9. Henry's constants, equipartition thicknesses, and selectivities for the processes of carbon dioxide and nitrogen adsorption and absorption in the ionic liquid, $[BMIM]^+[PF_6]^-$, from binary gas mixtures.

T, K	Henry's constant		Equipartition thickness, *nm*	Ideal selectivity	
	Bulk IL, $MPa \cdot nm^3$	Surface of IL, $MPa \cdot nm^2$		Bulk IL	Surface of IL
Adsorption of CO_2 from ternary mixtures of ionic liquid, carbon dioxide and nitrogen					
298	1.909 ± 0.035	0.757 ± 0.017	2.522 ± 0.104		
323	2.915 ± 0.089	1.236 ± 0.024	2.358 ± 0.117		
343	3.785 ± 0.078	1.700 ± 0.027	2.226 ± 0.080	83.051 ± 7.146	5.159 ± 0.539
393	6.961 ± 0.136	3.372 ± 0.039	2.064 ± 0.064	37.065 ± 4.385	4.668 ± 0.299
Adsorption of N_2 from ternary mixtures of ionic liquid, carbon dioxide and nitrogen				27.842 ± 3.482	4.320 ± 0.330
				12.568 ± 0.890	3.593 ± 0.283
298	159 ± 11	3.906 ± 0.319	40.591 ± 6.062		
323	108 ± 9	5.772 ± 0.259	18.721 ± 2.485		
343	105 ± 11	7.345 ± 0.448	14.348 ± 2.375		
393	87 ± 4	12.114 ± 0.815	7.222 ± 0.856		

For the equipartition thickness and selectivity we provide three digits after the decimal place to show that equation (9) in the main text provides equality between two ratios.

11. References

1. B. Doherty, X. Zhong, S. Gathiaka, B. Li and O. Acevedo, *J. Chem. Theory Comput.*, 2017, **13**, 6131-6145.

2. W. Fan, Q. Zhou, J. Sun and S. J. Zhang, *Chem. Eng. Data*, 2009, **54**, 2307-2311.

3. H. Tokuda, K. Hayamizu, K. Ishii, M. Susan and M. Watanabe, *J. Phys. Chem. B*, 2004, **108**, 16593-16600.

4. M. Freire, P. Carvalho, A. Fernandes, I. Marrucho, A. Queimada and J. Coutinho, *J Colloid Interface Sci.*, 2007, **314**, 621-630.

5. M. J. Abraham, T. Murtola, R. Schulz, S. Páll, J. C. Smith, B. Hess and E. Lindahl, *SoftwareX*, 2015, **1-2**, 19-25.

6. L. Martínez, R. Andrade, E.G. Birgin and J.M. Martínez, *Journal of Computational Chemistry*, 2009, **30**, 2157-2164.

7. L. B. Partay, G. Hantal, P. Jedlovszky, A. Vincze and G. Horvai, *J. Comput. Chem.*, 2008, **29**, 945-956.

8. M. Jorge, P. Jedlovszky and M. N. D. S. Cordeiro, *J. Phys. Chem. C*, 2010, **114**, 11169-11179.

9. M. Jorge, G. Hantal, P. Jedlovszky and M. N. D. S. Cordeiro, *J. Phys. Chem. C*, 2010, **114**, 18656-18663.

10. J. L. Anthony, E. J. Maginn and J. F. Brennecke, *J. Phys. Chem. B.*, 2002, **106**, 7315-7320.

11. D. Camper, P. Scovazzo, C. Koval and R. Noble, *Industrial & Engineering Chemistry Research*, 2004, **43**, 3049-3054.

12. I. Urukova, J. Vorholz and G. Maurer, *The Journal of Physical Chemistry B*, 2005, **109**, 12154-12159.

13. J. Jacquemin, P. Husson, V. Majer and M. F. Costa Gomes, *Fluid Phase Equilibria*, 2006, **240**, 87-95.

14. M. J. Muldoon, S. N. Aki, J. L. Anderson, J. K. Dixon and J. F. Brennecke, *The Journal of Physical Chemistry B*, 2007, **111**, 9001-9009.

15. D-Y. Peng and D. B. Robinson, *Ind. Eng. Chem. Fundamen.*, 1976, **15**, 59-64.

16. J. J. Potoff and J. I. Siepmann, *AIChE Journal*, 2001, **47**, 1676-1682.

17. C. G. Aimoli, E. J. Maginn and C. R. A. Abreu, *Fluid Phase Equilibria*, 2014, **368**, 80-90.